Mid-latitude Geomagnetic Indices "ASY" and "SYM" for 2009 (Provisional)

1. Introduction

To describe the geomagnetic disturbance fields in mid-latitudes with high-time (i.e. 1 minute) resolution, a longitudinally asymmetric (ASY) and a symmetric (SYM) disturbance index are introduced and derived for both H and D components, that is, for the components in the horizontal (dipole pole) direction H (SYM-H, ASY-H) and in the orthogonal (East-West) direction D (SYM-D, ASY-D). The symmetric disturbance field in H, SYM-H, is essentially the same as Sugiura's hourly Dst index (Sugiura and Poros, 1971), although we use 1 minute values from different sets of stations and a slightly different coordinate system. Similarly, the ASY-H asymmetric disturbance component in H is close to the asymmetric indices proposed by Kawasaki and Akasofu (1971), Crooker and Siscoe (1971), or Clauer et al.(1983). The ASY-D used in this data book was introduced and discussed in Iyemori (1990, 1996). It has been shown that the variation of the asymmetric H component correlates well with the AE index (e.g. Crooker, 1972; Clauer and McPherron, 1980). The results of an examination of the correlation between the ASY-D and the AE indices or the IMF-Bz and a discussion of the meaning of these indices will be published in somewhere else. Although there exists rather a good correlation between both ASYs and the AE indices, it should be noted that there are some essential differences between them and we should be careful when we use the ASY indices as a monitor of disturbances in the polar region.

2. Method of derivation

Shown in Table 1 and Figure 1 are a listing of geomagnetic observatories used here and their distribution in the geomagnetic dipole coordinate system respectively. It should be noted that some of the stations used here (i.e. Urumqi, Fredericksburg, Boulder, Tucson, Memambetsu, Martin de Vivies and Chambon- la-Foret) are at higher latitudes than those used in the derivation of Sugiura's standard Dst index (i.e. Honolulu, Kakioka, Alibag, Hermanus and San Juan). Only six of the stations are used for the derivation of each month, some stations being replaced by others depending on the availability and the condition of the data of the month. The combination of stations used is shown on the frame of each plot. The data are processed in units of one month. Therefore some gap in the magnitude is seen between successive months. The derivation procedure essentially consists of the following four steps:

(1) Subtraction of the geomagnetic main field and the Sq (solar quiet daily variation) field to calculate the disturbance field component.

(2) Coordinate transformation to a dipole coordinate system.

(3) Calculation of the longitudinally symmetric component (i.e. six station average) and the asymmetric component (i.e. disturbance field minus the symmetric component).

(4) Derivation of the asymmetric indices (i.e. the range between the maximum and the minimum asymmetric fields).

A detailed description of the derivation and the characteristics of the indices will appear elsewhere. The following is a rough explanation of each step of the derivation.

TABLE 1.

STATION NAME	ABB CODE	G.G. LAT.	G.G. LONG.	G.M. LAT.	G.M. LONG.	INVARIANT LAT.	ROTATION ANGLE
San Juan	SJG	18.110	293.850	28.04	6.54	32.5	-8.9
Fredericksburg	FRD	38.200	282.630	48.14	353.93	50.4	0.4
Boulder	BOU	40.130	254.760	48.24	321.28	49.1	2.5
Tucson	TUC	32.170	249.270	39.73	316.74	39.7	2.7
Honolulu	HON	21.320	202.000	21.71	270.27	20.2	0.5
Memambetsu	MMB	43.910	144.189	35.63	211.74	34.9	-16.1
Urumqi	WMQ	43.800	87.700	34.34	162.53	36.5	7.66
Alibag	ABG	18.638	72.872	10.37	146.55	–	6.8
Martin de Vivies	AMS	-37.796	77.574	-46.22	144.93	48.6	-32.4
Hermanus	HER	-34.425	19.225	-34.08	84.63	43.6	-10.1
Chambon-la-Foret	CLF	48.025	2.261	49.75	85.80	45.7	13.6

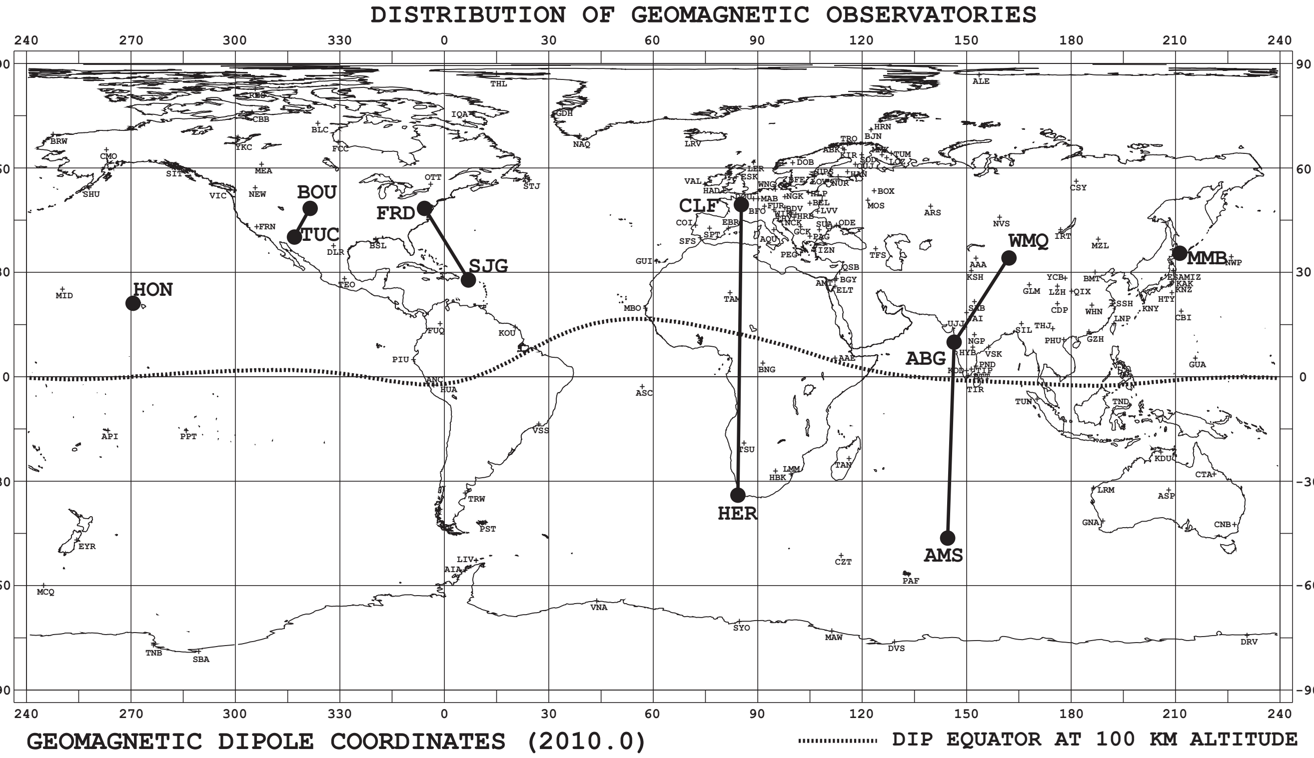

Figure 1. Data are obtained at the observatories shown by the solid circles.
The stations replaced with each other are connected by solid lines.

(1) Subtraction of the main field and the Sq field

The geomagnetic field consists of the main field, the solar quiet daily variation and the disturbance field. To get the disturbance field, the geomagnetic main field and the Sq field have to be subtracted. To calculate the base value including the Sq field, the data of international five quiet days are used. That is, the original data of the international 5-Q days of the month that include the Sq field as well as the geomagnetic main field are averaged every minute and fitted by B-spline functions. For some special cases where some of the 5-Q days are not suitable for the purpose because of missing data etc., another quiet day is selected from international 10 quiet days of the month. The period used for the quiet days is marked by the symbol 'Q' in the hourly value tables. The fitted values are then subtracted from original data to get the disturbance component.

(2) Coordinate transformation

In a geomagnetic storm period, the ring current is the main source of the disturbance field in the H component observed at mid-latitudes. As the ring current flows in the magnetosphere at a distance of several Re (radius of the Earth) and in the equatorial plane, its geomagnetic effect should be nearly parallel to the dipole axis. On the other hand, the H direction at each observatory is generally different from the dipole pole direction because of the non-dipole component or local geomagnetic anomalies. Therefore the ring current effect is mixed into the D component. To minimize the ring current effect in the D-component, the data are transformed to the dipole coordinate system at each station. The differences between the dipole pole position and local geomagnetic direction are shown in Table 1.

(3) Calculation of the symmetric components SYM-H and SYM-D

The longitudinally symmetric component is calculated by averaging the disturbance component at each minute for the 6 stations. For the H component, a latitudinal correction is made on the averaged value to get the value (SYM-H) which corresponds to Sugiura's equatorial Dst index, that is, it is divided by the 6-station average of $\cos\theta_m$, where θ_m is the dipole latitude of each station, though the stations used, the coordinate system and the method to subtract the base value with Sq current effect are different from his method of derivation. On the symmetric component of D (SYM-D), we make no latitudinal correction at all.

(4) Calculation of the asymmetric disturbance indices, ASY-H and ASY-D

The asymmetric component at each station is obtained by subtracting the symmetric component from each disturbance field. For the H component, the symmetric part is subtracted after making a latitudinal correction assuming that the SYM-H represents the magnitude of the uniform field parallel to the dipole axis generated by the ring current. After subtracting the symmetric part, a latitudinal correction is made by multiplying the normalization coefficient for each station which is determined empirically as the standard deviations of the asymmetric variation for the 6 stations become equal.

The ASY-H and the ASY-D indices are defined as the range between the maximum and the minimum deviation at each moment for the H and the D component, respectively.

3. Explanation of the plots and hourly tables

Each frame of the plots in this data book covers a period of two days. The upper panel shows, from top to bottom, ASY-D, ASY-H (positive downward), SYM-D (thin line) and SYM-H (thick line). The lower panel shows the magnetic local time where the maximum (+) and minimum (-) asymmetric deviations are observed. For periods when one or more stations have no data, a dark bar with height proportional to the number of stations with missing data, is drawn at the bottom of the panel. A storm sudden commencement (SSC) and the start time of a solar flare effect (SFE) are indicated by solid and open triangles, respectively. The SSCs and SFEs are taken from the Solar Geophysical Data published by NOAA/NGDC. Cases where the highest quality of the SSC reported is 'C' or only one station reports an SFE are not indicated here. Therefore there may be many SSCs and SFEs not indicated by the symbols on these plots.

The hourly averaged value of the ASY-D and ASY-H indices are tabulated every month. The hourly SYM-H index is not tabulated to avoid confusion with the hourly Dst index. Instead of the tables of the SYM-H index, a comparison (i.e. the correlation plots) between the hourly SYM-H and the Quick-Look Dst index is shown in Figures 3 (a) - (b). The hourly SYM-D index is also not tabulated because the stations are insufficiently well distributed to properly treat the symmetric disturbance of the D component. The quiet days used for the calculation of the base line are marked by a symbol 'Q'. Most of the days correspond to the international 5-quiet days.

4. Comparison with the AE indices and the Dst index

Figures 2-a and 2-b are examples of a comparison between the ASY and SYM indices and the auroral electrojet indices, AE. Figure 2-a shows a rather disturbed period and Figure 2-b shows a moderately disturbed period. From these plots, the qualitative similarities and the differences between the ASY and AE indices can be seen. The main qualitative differences are seen in the spectral characteristics and in the sensitivity to minor substorm activity. The ASY indices are more smoothly varying and it is rather difficult for them to reflect minor substorm activity in the polar region. A quantitative comparison will appear elsewhere. Users should be aware that the ASY indices should not be used as substitutes for the AE indices, although there are some similarities between them.

A comparison of the hourly SYM-H index with the Quick-Look Dst index is shown in Figures 3a and 3b. We see some offset between the two indices which come from the difference in the method to determine the base values. The base value at each station is more carefully determined for the hourly Dst index taking into account the geomagnetic secular variation than for this provisional SYM-H index. The main difference between the 1 minute SYM-H and the hourly Dst index is the time resolution, and the effects of the solar wind dynamic pressure variation are more clearly seen in the SYM-H than in the hourly Dst index.

5. Future improvements

The indices plotted in this data book are provisional in the sense that the combination of the

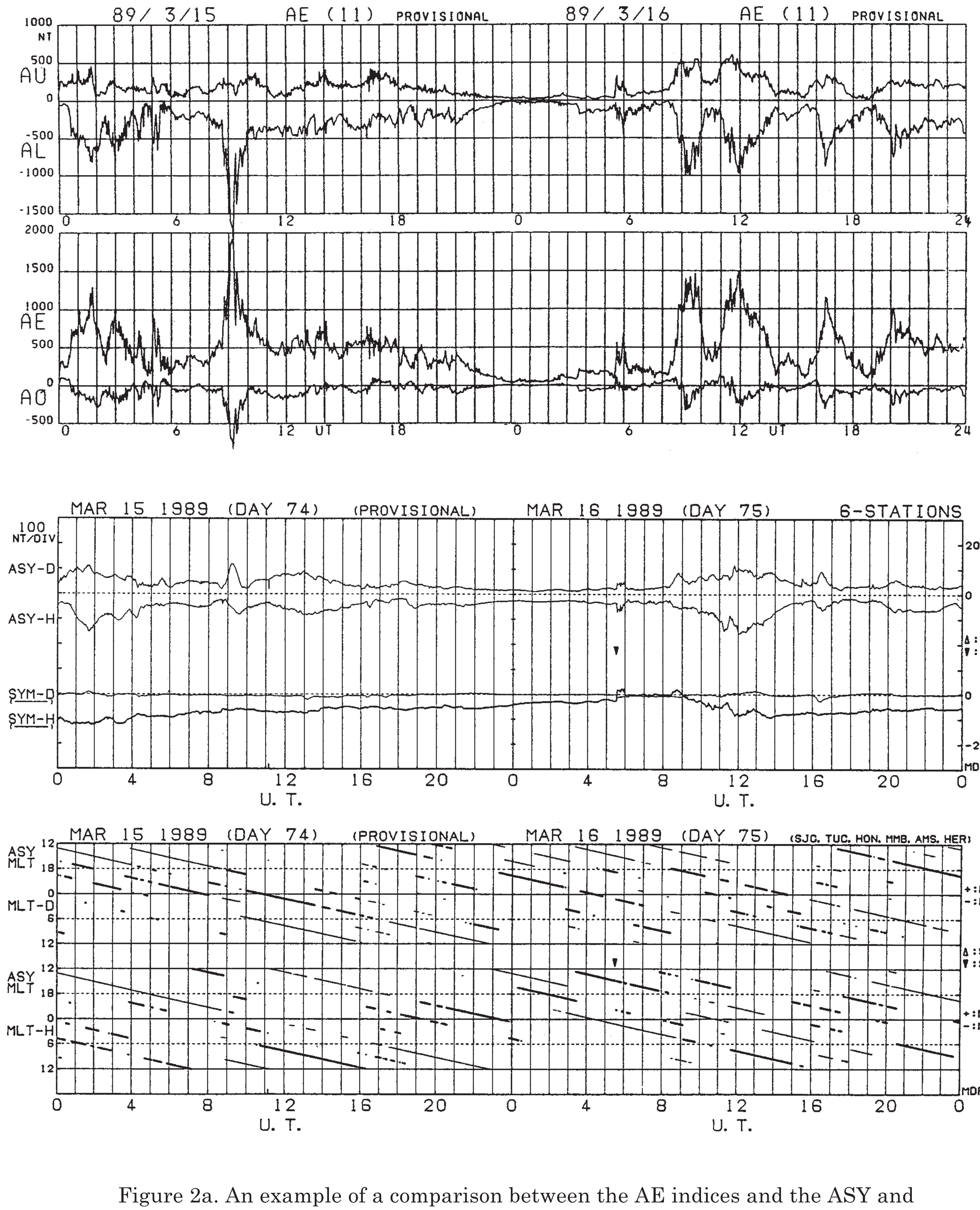

Figure 2a. An example of a comparison between the AE indices and the ASY and SYM indices of rather disturbed period. An SSC is indicated by a solid triangle. The magnetic local time at the station which gives the maximum or the minimum asymmetric deviation from symmetric disturbance is shown by a symbol + (thick line) or a symbol - (thin line), respectively.

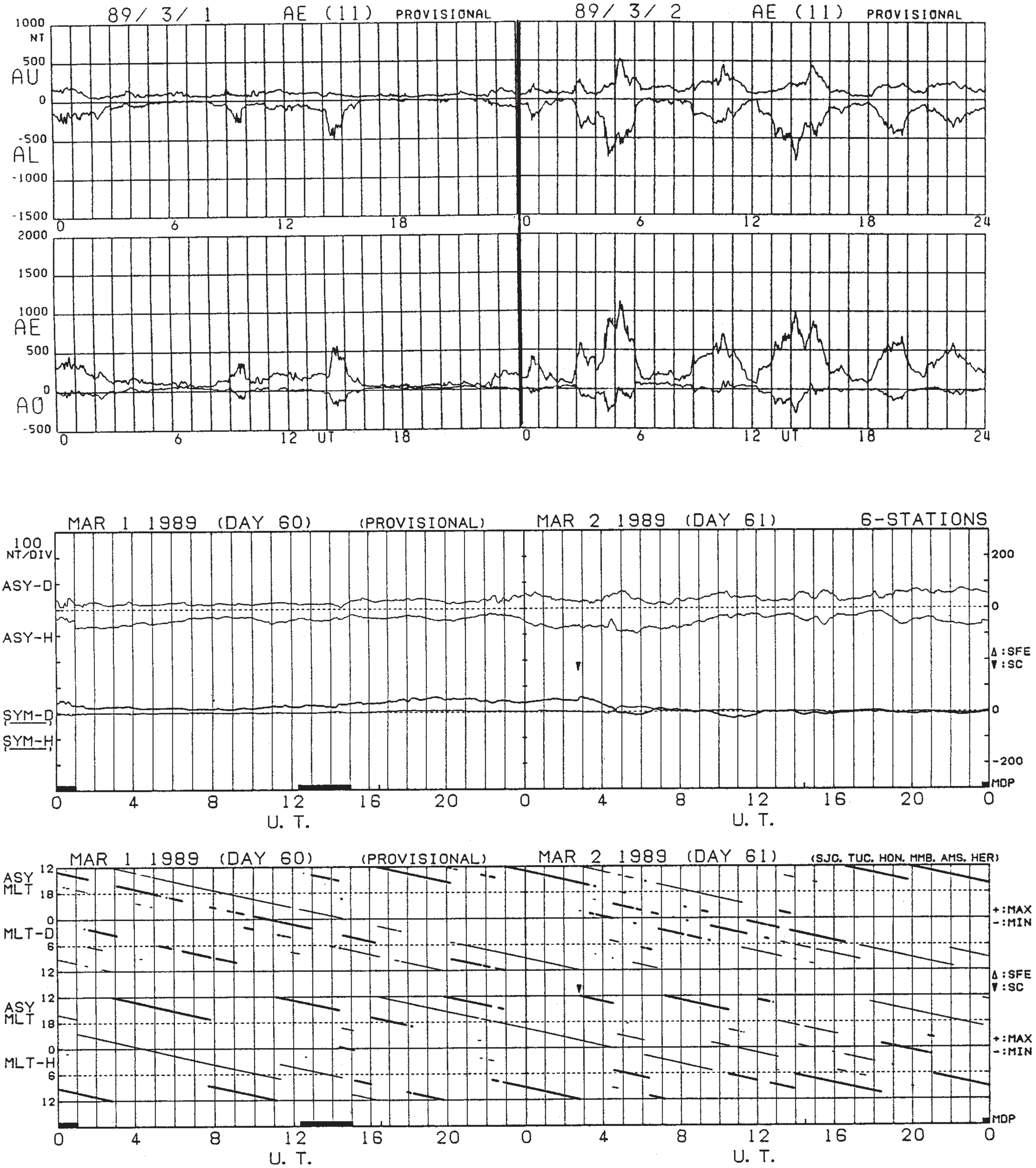

Figure 2b. An example of a comparison between the AE indices and the ASY and SYM indices of moderately disturbed period. The missing data periods are shown by the dark bars at the bottom of the panel. The height of the bars is proportional to the number of stations (1 station in this case) with missing data period (MDP).

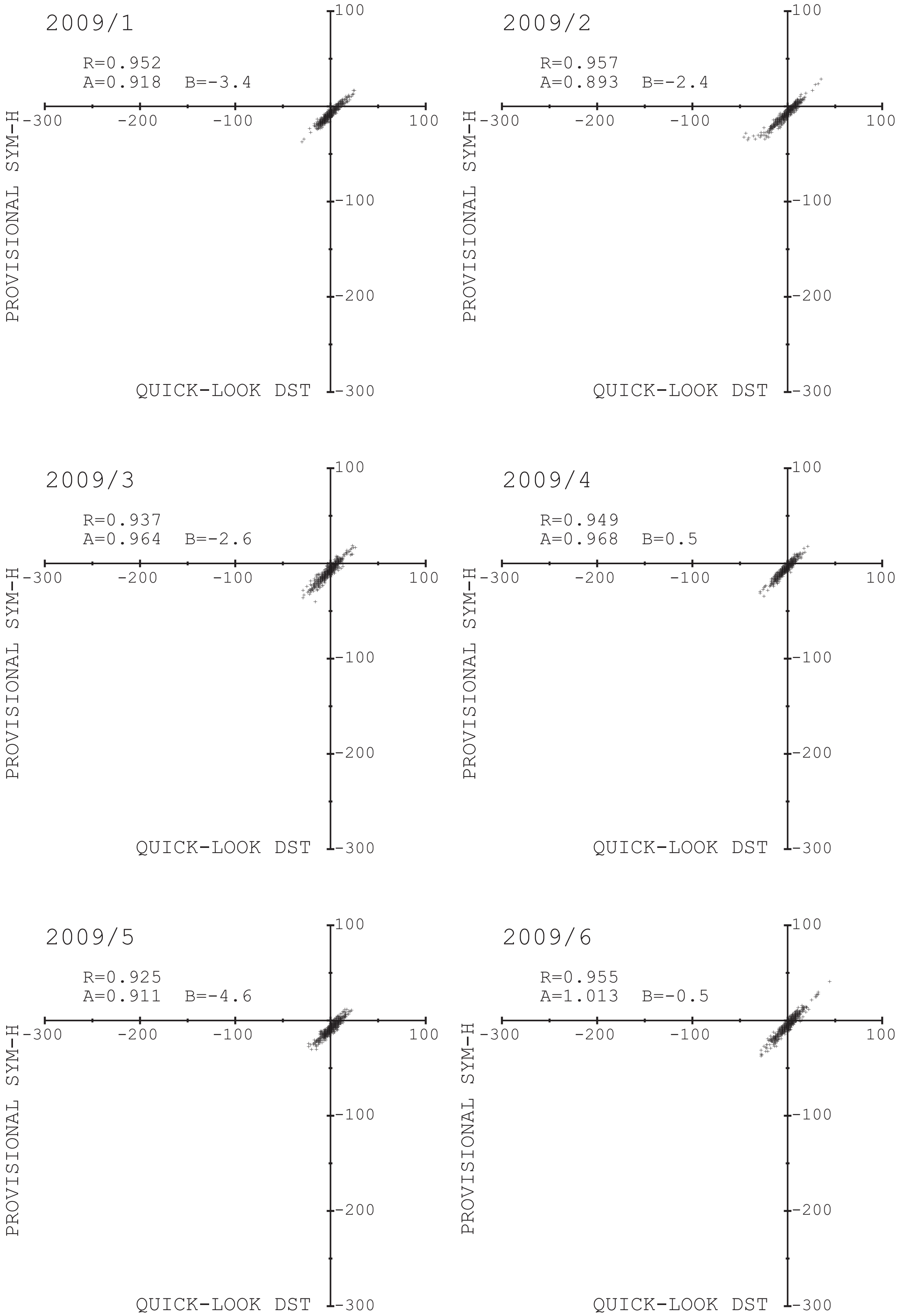

Figure 3a. Correlation plots between the hourly averaged SYM-H and the Quick-Look Dst for January-June, 2009. The correlation coefficients R, the parameters of the regression line A and B (i.e. SYM-H=A*Dst+B) are shown on each panel.

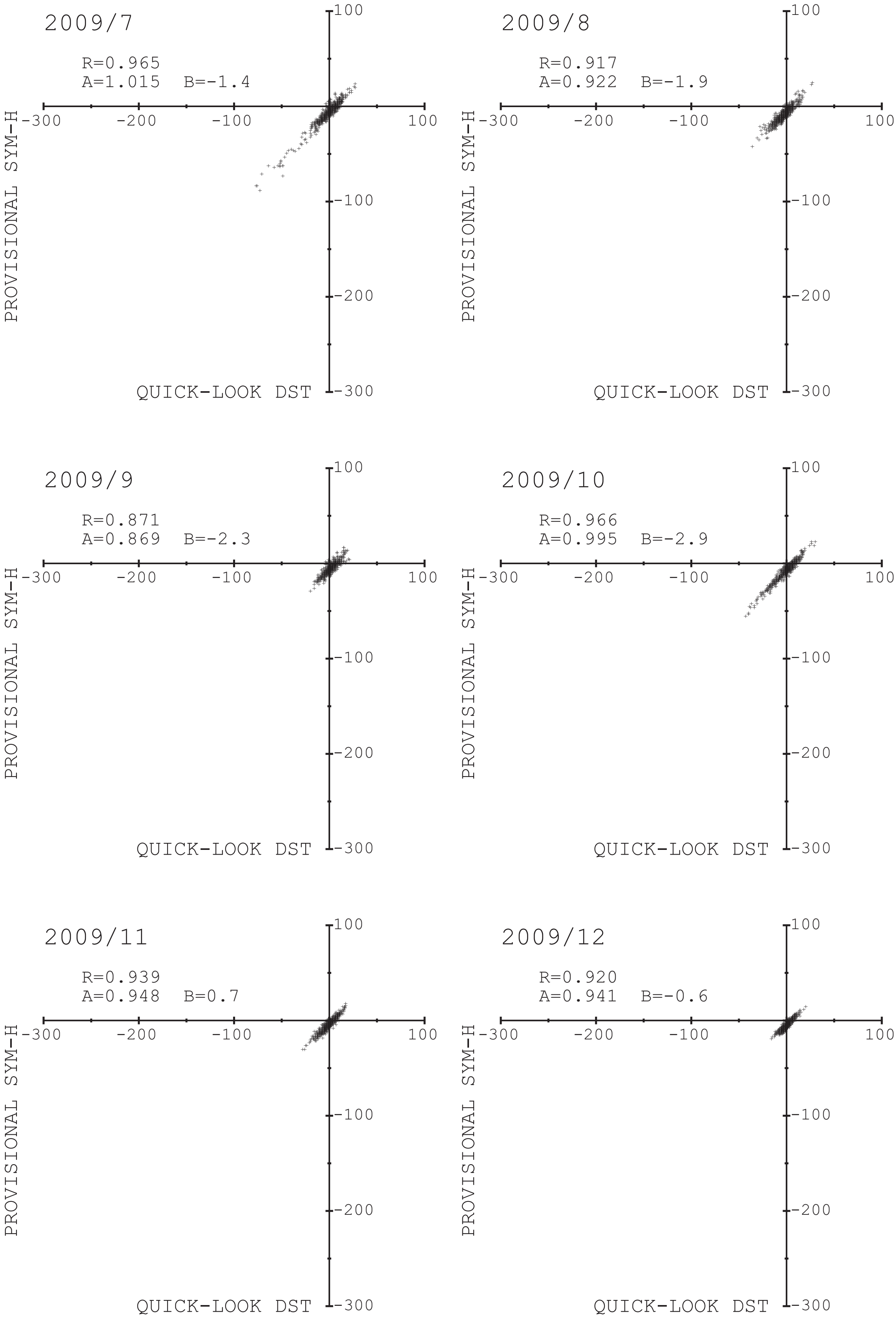

Figure 3b. Correlation plots between the hourly averaged SYM-H and the Quick-Look Dst for July-December, 2009.

stations could be changed in future to get more stable results with minimum universal time and seasonal dependence. It is necessary to continue the provisional derivation of the indices for some more years until the optimal method and the best combination of stations are established. The availability of the digital data could be changed and it will also be necessary to try to get the digital geomagnetic data from more suitable locations. Modification of the procedure for real-time derivation may also be necessary in future.

6. Post-Script files of the plots and WWW homepage service

The Post-Script files of the plots shown in the latest issue are available from our web page.
The URL is:

http://wdc.kugi.kyoto-u.ac.jp/asyplot/

Plots with the AE indices for the period when the AE indices have been derived are also available from:

http://wdc.kugi.kyoto-u.ac.jp/

Acknowledgments

The data used in this data book were kindly provided by the U.S. Geological Survey (HON, BOU, FRD, SJD, and TUC) through the World Data Center for STP, Boulder, the Hermanus Magnetic Observatory (HER), the Chambon-la-Foret Magnetic Observatory (CLF), Institut de Physique du Globe de Strasbourg (AMS), the Kakioka Magnetic Observatory (MMB), the Indian Institute of Geomagnetism (ABG), the Urumqi Geomagnetic Observatory, Seismological Bureau of Xinjiang Uygur Autonomous Region (WMQ).
The compilation of the geomagnetic data and publication of this data book have been supported in part by grant 208041 and 218046 under the Japan Society for Promotion of science (JSPS).

T. Iyemori, M. Takeda, M. Nose, Y. Odagi and H. Toh
Data Analysis Center for Geomagnetism and
Space Magnetism, Graduate School of Science,
Kyoto University, Kyoto 606-8502, Japan.
TEL: 81-75-753-3929
FAX: 81-75-722-7884
E-MAIL: iyemori@kugi.kyoto-u.ac.jp
WWW: http://wdc.kugi.kyoto-u.ac.jp/

(February 2010)

References

Clauer, C.R. and R.L. McPherron, The relative importance of the interplanetary electric field and magnetospheric substorms on the partial ring current development, J. Geophys. Res., 85, 6747-6759, 1980.

Clauer, C.R., McPherron, R.L. and C. Searls, Solar wind control of the low- latitude asymmetric magnetic disturbance field, J. Geophys. Res., 88, 2123-2130, 1983.

Crooker, N.C. and G.L. Siscoe, A study of the geomagnetic disturbance field asymmetry, Radio Sci., 6, 495-501, 1971.

Crooker, N.C., High-time resolution of the low-latitude asymmetric disturbance in the geomagnetic field, 77, 773-775, 1972.

Iyemori, T., Storm-time magnetospheric currents inferred from mid-latitude geomagnetic field variations, J. Geomag. Geoelectr., 42, 1249-1265, 1990.

Iyemori, T. and D.R.K. Rao, Decay of the Dst field of geomagnetic disturbance after substorm onset and its implication to storm-substorm relation, Ann. Geophys., 14, 608-618, 1996.

Kawasaki, K. and S.-I. Akasofu, Low-latitude DS component of geomagnetic storm field, J. Geophys. Res., 76, 2396-2405, 1971.

Sugiura, M. and D.J. Poros, Hourly values of equatorial Dst for years 1957 to 1970, Rep. X-645-71-278, Goddard Space Flight Center, Greenbelt, Maryland, 1971.